

Efflorescence Relative Humidity of Mixed Sodium Chloride and Sodium Sulfate Particles

Yonggang Gao,[†] Liya E. Yu,[‡] and Shing Bor Chen^{*,†}

Department of Chemical and Biomolecular Engineering and Division of Environmental Science and Engineering, National University of Singapore, Singapore 117576

Received: April 25, 2007; In Final Form: July 17, 2007

We study the efflorescence relative humidity (ERH) of particles composed of sodium chloride and sodium sulfate. Both experimental and theoretical investigations are conducted to explore the effects of particle size and mixing ratios between two inorganic materials on ERH. A previously developed theoretical model (Gao et al. *J. Phys. Chem. A* 2006, 110, 7602; ref 1) is applied as the framework to build a formulation assuming that one salt nucleates much faster than the other, and the critical nuclei formation of the former controls the rate of efflorescence. The predicted ERHs agree favorably with the experimental data, except for particles containing Na₂SO₄ in a mole fraction of around 0.25. At this composition, our model underestimates the ERH, indicating certain factors involved in the efflorescent processes that are overlooked in our formulation. Relative to particles larger than 40 nm, the Kelvin effect more significantly affects particles smaller than this size.

1. Introduction

Inorganic salts account for 25~50% of fine aerosol mass.² Since atmospheric particulates contain a complicated chemical composition, understanding deliquescent and efflorescent behaviors of multicomponent particles is important to elucidate their effects on air quality, visibility degradation, and climate change.³ Deliquescent behavior of particles composed of multicomponents, such as NaCl–Na₂SO₄, NH₄Cl–NH₄NO₃, NaCl–NaNO₃, and Na₂SO₄–(NH₄)₂SO₄, has been investigated experimentally^{4–7} and theoretically.^{8–11} Among these studies, two types of deliquescence relative humidity (DRH) of the multicomponent particles are reported: (1) the mutual deliquescence relative humidity (MDRH) at which solid particles partially dissolve in the absorbed water and (2) the complete deliquescence relative humidity (CDRH) at which particles complete deliquescence and become homogeneous airborne droplets. The MDRH is lower than the minimum DRH of all components in their individual pure solutions and is independent of the particle composition. Unlike MDRH, CDRH depends substantially on the fractions of individual components in mixtures.

Efflorescence of a multicomponent particle is more complicated than that of a single component particle. The latter involves only homogeneous nucleation, whereas additional heterogeneous nucleation may occur for the former. Schlenker et al.¹² reported that ammonium bisulfate or ammonium nitrate, which cannot crystallize in its pure solution (no efflorescence relative humidity (ERH)), actually crystallize through heterogeneous nucleation in a multicomponent solution after crystals of other species are formed through homogeneous nucleation. Ge et al.¹³ investigated the chemical composition of particles dried from KCl–NaCl, KI–KCl, and (NH₄)₂SO₄–NH₄NO₃ mixture solutions at different mole ratios using rapid single-particle mass spectrometry (RSMS). They found that a dried multicomponent particle

consists of a pure salt surrounded by mixed salt coating, and the core–shell arrangement depends on the salt mixing ratios. These two studies suggest that homogeneous nucleation plays a key role in the crystallization of a multicomponent solution. For the ensuing heterogeneous nucleation of other salts, the formed crystal of the first salt must be sufficiently large to act as a heterogeneous inclusion.¹⁴ The necessity of a sufficiently large crystal is supported by the observed decrease in ERH of NH₄NO₃ when the crystal size becomes too small.¹⁵ Since both ensuing heterogeneous nucleation and crystal growth occur rapidly, one can assume that the formation of the critical nuclei of the first salt controls the rate of efflorescence. Accordingly, homogeneous nucleation theory may be promising for ERH prediction of a particle consisting of more than one salt. This approach has been applied to investigate how H₂SO₄, which cannot crystallize, affects ERH of (NH₄)₂SO₄.¹¹

In this paper, we attempt to predict the ERH of binary mixed salt particles using homogeneous nucleation theory. NaCl and Na₂SO₄ were selected as tested components because (1) these two salts exhibit distinctive ERHs, 58% RH for Na₂SO₄ and 48% RH for NaCl, facilitating observations of changes in resultant ERH and (2) available experimental data of micrometer-sized particles containing these two salts at various mixing ratios^{4,6,7} provide a basis to further verify our theoretical prediction for particles of the micrometer size. We modified the theoretical model previously developed for a single salt particle¹ to apply to binary NaCl–Na₂SO₄ particles and then present the trend in ERH of NaCl–Na₂SO₄ particles. ERH measurements for NaCl–Na₂SO₄ particles down to 40 nm were conducted to verify our theoretical calculations. To the best of our knowledge, this is the first theoretical investigation on the ERH of mixed NaCl–Na₂SO₄ particles with different mixing ratios supported with experimental data.

2. Theories and ERH Prediction

To facilitate theoretical analysis, we hypothesize that the rate of the crystallization process at ERH of a droplet of mixed NaCl and Na₂SO₄ solutions is mainly controlled by homogeneous

* To whom correspondence should be addressed. E-mail: checsb@nus.edu.sg.

[†] Department of Chemical and Biomolecular Engineering.

[‡] Division of Environmental Science and Engineering.

TABLE 1: Physical Properties of Na₂SO₄ and NaCl

parameters	Na ₂ SO ₄	NaCl
v_c (m ³)	8.8×10^{-29}	4.48×10^{-29}
ρ_{salt} (kg/m ³) ^a	2680	2165
M_{salt} (g/mol)	142.0	58.44
$m_{\text{saturation}}$ (mol/kg) ^b	1.978	6.143

^a Obtained from Lide et al.²¹ ^b Calculated values according to the solubility reported by Lide et al.²¹

nucleation of one salt. This hypothesis is discussed in detail based on comparison between theoretical prediction and experimental data in the next section. Following our prior formulation,¹ the nucleation rate at an RH is calculated by

$$J = J_0 e^{-\Delta G_h^*/K_B T} \quad (1)$$

where

$$\Delta G_h^* = \frac{16\pi\sigma_{\text{drop-nuc}}^3 v_c^2}{3(K_B T \ln S)^2} \quad (2)$$

is the Gibbs energy barrier, and the prefactor J_0 is estimated to be $2.8 \times 10^{38} \text{ m}^{-3} \text{ s}^{-1}$ for NaCl and 1.7×10^{38} for Na₂SO₄ by applying the method of Richardson and Snyder¹⁶ and Onasch et al.¹⁷ In eq 2, v_c is the volume of a NaCl or Na₂SO₄ molecule; $K_B T$ is the thermal energy; $S = a/a_0$ is the supersaturation ratio between a and a_0 , representing solute activity in supersaturated and saturated mixed salt solutions, respectively; and $\sigma_{\text{drop-nuc}}$ is the interfacial tension between a NaCl or Na₂SO₄ nucleus and the supersaturated mixed salt solution. The nucleation rate J_c at the ERH can be estimated by

$$J_c = \frac{1}{V_e t} \quad (3)$$

where V_e is the corresponding volume of the supersaturated droplet of the mixed salt solution, and t is the nucleation induction time.^{17,18} Because the actual induction time is difficult to measure, we adopted the estimated residence time for t according to experimental setup and flow rate for particle efflorescence. Since the employed residence time could be longer than the actual induction time, the predicted ERH could be overestimated.

To determine the nucleation rate and ERH, one needs to calculate various thermodynamic properties. Let the subscripts w , α , and β denote water, NaCl, and Na₂SO₄, respectively. Given a spherical dry particle consisting of the two salts with mass equal to W_α and W_β , we assume simple volume additivity^{19,20} to determine the diameter D_0 and density ρ_{dry} of dry particles using the individual crystal densities as shown in Table 1. For a droplet resulting from water uptake and salt dissolution, we can determine the salt molalities m_α and m_β by specifying the water activity and using the Zdanovskii–Stokes–Robinson (ZSR) relationship,²²

$$\frac{m_\alpha}{m_{\alpha,0}(a_w)} + \frac{m_\beta}{m_{\beta,0}(a_w)} = 1 \quad (4)$$

where $m_{i,0}(a_w)$ is the molality for the corresponding single-salt solution with the same water activity a_w . Equation 4 has been commonly employed by many researchers.^{5,9,10,23} The correlations for $m_{i,0}(a_w)$ are given in the Appendix. The total salt molality is hence $m = m_\alpha + m_\beta$, and the water mass W_w can be

calculated from the molality and molecular weight of either salt. The density ρ of the mixed salt solution is estimated by⁴

$$\frac{1}{\rho} = \frac{1}{(W_\alpha + W_\beta)} \left(\frac{W_\alpha}{\rho_\alpha} + \frac{W_\beta}{\rho_\beta} \right) \quad (5)$$

where ρ_i is the density of the corresponding single-salt solution with molality m . The correlations for ρ_i are given also in the Appendix. The growth factor defined as the diameter ratio of wet to dry particle is

$$GF = \frac{D}{D_0} = \left[\frac{\rho_{\text{dry}}(W_w + W_\alpha + W_\beta)}{\rho(W_\alpha + W_\beta)} \right]^{1/3} \quad (6)$$

Note that sodium sulfate in a mixed-salt solution crystallizes to anhydrous salt (Na₂SO₄), because a supersaturated solution droplet under ambient conditions rarely crystallizes to the decahydrate, Na₂SO₄·10H₂O.^{19,24}

The NaCl and Na₂SO₄ activities in the mixed-salt solution are calculated by

$$a_\alpha = (\gamma_\alpha m_\alpha)^2 \quad (7)$$

$$a_\beta = 4(\gamma_\beta m_\beta)^3 \quad (8)$$

where γ_i is the activity coefficient of salt i . According to Bromley,²⁵ the activity coefficient can be calculated by

$$\log \gamma_\alpha = -A_\gamma \frac{z_1 z_2 I^{1/2}}{1 + I^{1/2}} + \frac{z_1 z_2}{z_1 + z_2} \left[\frac{F_1}{z_1} + \frac{F_2}{z_2} \right] \quad (9)$$

$$\log \gamma_\beta = -A_\gamma \frac{z_1 z_3 I^{1/2}}{1 + I^{1/2}} + \frac{z_1 z_3}{z_1 + z_3} \left[\frac{F_1}{z_1} + \frac{F_3}{z_3} \right] \quad (10)$$

where the subscripts 1, 2, and 3 represent Na⁺, Cl⁻, and SO₄²⁻, respectively. z_i is the absolute charge number of ion species i , and A_γ is the Debye–Huckel constant equal to $0.511 \text{ kg}^{1/2} \text{ mol}^{-1/2}$ at 298.15 K. The functions in eqs 9 and 10 are given by

$$F_1 = X_{21} \log \gamma_{12}^0 + X_{31} \log \gamma_{13}^0 + \frac{A_\gamma I^{1/2}}{1 + I^{1/2}} (z_1 z_2 X_{21} + z_1 z_3 X_{31}) \quad (11)$$

$$F_2 = X_{12} \log \gamma_{12}^0 + \frac{A_\gamma I^{1/2}}{1 + I^{1/2}} z_1 z_2 X_{12} \quad (12)$$

$$F_3 = X_{13} \log \gamma_{13}^0 + \frac{A_\gamma I^{1/2}}{1 + I^{1/2}} z_1 z_3 X_{13} \quad (13)$$

with

$$X_{ij} = \left(\frac{z_i + z_j}{2} \right) \frac{m_i}{I} \quad (14)$$

where

$$I = \frac{1}{2} \sum_{i=1}^3 m_i z_i^2$$

is the ionic strength, and γ_{ij}^0 is the mean ionic activity coefficient of the pair i – j (binary activity coefficient) for a solution containing only i and j ions at I equal to that of the

mixed salt solution. The binary activity coefficient γ_{ij}^0 is calculated from equations of Kusik and Meissner,²⁶

$$C = 1 + 0.055q \exp(-0.023I^3) \quad (15)$$

$$\log \Gamma^* = \frac{-0.5107I^{1/2}}{1 + CI^{1/2}} \quad (16)$$

$$B = 0.75 - 0.065q \quad (17)$$

$$\Gamma^0 = [1 + B(1 + 0.1I)^q - B]\Gamma^* \quad (18)$$

$$\log \gamma_{ij}^0 = z_i z_j \log \Gamma^0 \quad (19)$$

where q is equal to 2.23 and -0.19 for NaCl and Na₂SO₄, respectively.²⁷ In order to calculate supersaturation ratio S in eq 2, the saturation activity of each salt in the mixed salt solution a_0 is assumed to take the value for the corresponding single-salt solution at the same temperature and pressure.²⁸

The interfacial tension between a critical nucleus of each salt and the supersaturated mixed salt solution ($\sigma_{\text{drop-nuc}}$) can be estimated using Young's equation with the assumption of a zero contact angle,¹¹ namely,

$$\sigma_{\text{drop-nuc}} = \sigma_{\text{nuc-air}} - \sigma_{\text{drop-air}}(m) \quad (20)$$

At a known m , the ionic strength of the mixed-salt solution can be written as $I = I_\alpha + I_\beta$, and $\sigma_{\text{drop-air}}$ is then calculated using the simple mixing rule:²⁹

$$\sigma_{\text{drop-air}} = y_\alpha \sigma_{\alpha,0} + y_\beta \sigma_{\beta,0} \quad (21)$$

where $y_\alpha = I_\alpha/I$, $y_\beta = I_\beta/I$, and $\sigma_{i,0}$ is the surface tension of the corresponding single salt solution at the same I . In this study, the formula of Pruppacher and Klett³⁰ is adopted to calculate the surface tension of a NaCl solution,

$$\sigma_{\alpha,0} = 0.072 + 0.0017m \quad (22)$$

The surface tension of a Na₂SO₄ solution is expressed by the formula of Li et al.,³¹

$$\sigma_{\beta,0} = \sigma_w - \frac{RT}{(V_w^2 N_A)^{1/3}} \ln a_w \quad (23)$$

where σ_w and V_w are the surface tension and molar volume of pure water, respectively, and N_A is Avogadro's constant. For each salt, $\sigma_{\text{nuc-air}}$ can be determined from the experimental measured ERH for the single-salt solution and the corresponding fitted $\sigma_{\text{drop-nuc}}$ and evaluated $\sigma_{\text{drop-air}}$. Accordingly, the calculated $\sigma_{\text{nuc-air}}$ are found to be 0.169 N/m for Na₂SO₄ and 0.197 N/m for NaCl.

Taking into account the Kelvin effect, the relative humidity is determined by

$$\text{RH} = 100 \times a_w \exp\left(\frac{4M_w \sigma_{\text{drop-air}}}{RT \rho_w D}\right) \quad (24)$$

where D is the droplet diameter, M_w and ρ_w the molar mass and density of water, R the molar gas constant, and T the absolute temperature.

To facilitate ERH prediction, we first calculate J_α and J_β for the two salts using eq 1 at various values of a_w . The ERH determination is then conducted by an iterative method developed in our prior work to ensure identical nucleation rates calculated from eqs 1 and 3. The flowchart is shown in Figure

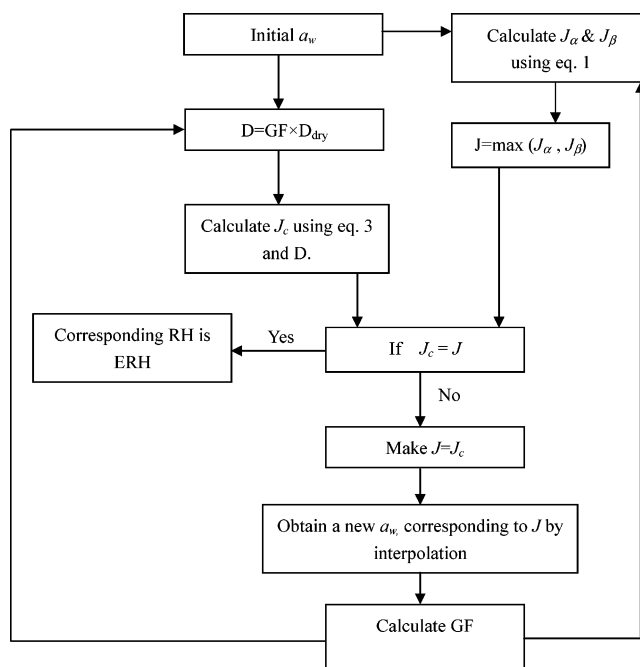


Figure 1. Flowchart for the calculation procedure of ERH.

1, and the prediction process starts with a randomly specified a_w (<0.7). At the given a_w , J_c , J_α , and J_β are calculated to check whether J_c equals $\max(J_\alpha, J_\beta)$. If the condition is met, the corresponding RH is ERH. Otherwise, a new a_w is obtained by interpolation. Such iteration is continued until J_c equals $\max(J_\alpha, J_\beta)$ within tolerance. We list some of the calculated quantities as functions of water activity for the case of a dry particle with diameter of 1 μm and the NaCl-to-Na₂SO₄ mole ratio of 1:1 in Table 2.

3. Experimental Section

To measure the ERH of airborne particles composed of mixed salts, we employed a tandem differential mobility analyzer (TDMA) system coupled with an exposure chamber, which was described in detail elsewhere.¹ In brief, prior to generation of airborne salt particles, the whole system was purged using purified dry air for more than an hour. To generate particles consisting of salt mixtures, solutions (0.1 wt % of salts) were prepared comprising NaCl (purity $>99.5\%$, Merck, Germany) and Na₂SO₄ (purity $>99\%$, Merck, Germany) in seven different molar proportions of 1:3, 1:2, 1:1, 2:1, 3:1, 4:1, and 9:1, in addition to pure NaCl (0% Na₂SO₄) and pure Na₂SO₄ (0% NaCl). To generate monodispersed particles, aerosolized salt particles were carried by compressed air through a neutralizer before they entered an electrostatic classifier (3080L, TSI Inc., USA). For individual batch measurements, droplets in monomodal distribution ($66-72 \pm 10$ nm) were introduced into the exposure chamber in a consistent flow rate (1 ± 0.01 L/min) for more than 10 min under 90% RH. Once the size distribution of salt droplets reached a steady state, RH in the exposure chamber was decreased by adjusting flow rates of dry air ($<5\%$ RH), varying from 0 to 2 L/min at room temperature. RH in the exposure tube was monitored using a thermohygrometer (Vaisala HMH45, Finland) with a precision of $\pm 2\%$ RH. Size of particles exiting the exposure tube was measured using a scanning mobility particle sizer (SMPS 3969, TSI Inc., USA), and effloresced dry particles remained in monomodal distribution with a size range of 40–49 nm (± 10 nm). Propagated errors of our experimental data, including the standard deviation of

TABLE 2: Calculated Physical Quantities with Varying Water Activity for the Case of a Particle with Dry Diameter of 1 μm and the NaCl-to- Na_2SO_4 Mole Ratio of 1:1 (Residence Time Is 15 min)

a_w	ρ (kg/m ³)	$\sigma_{\text{drop-air}}$ (N/m)	GF	$\sigma_{\text{drop-nuc},\beta}$ (N/m) ^a	J_β (m ⁻³ s ⁻¹)	$\sigma_{\text{drop-nuc},\alpha}$ (N/m) ^b	J_α (m ⁻³ s ⁻¹)	RH (%)
0.801	1323.79	0.080 56	1.765	0.088 44	0	0.1159	no ^d	80.2
0.701	1402.31	0.084 28	1.6275	0.084 72	2.0×10^{-140}	0.1122	no ^d	70.2
0.601	1512.56	0.091 83	1.4841	0.077 17	2.7×10^{-15}	0.1047	no ^d	60.2
0.581	1540.97	0.093 72	1.4536	0.075 28	1.8×10^{-3}	0.1028	no ^d	58.2
0.571	1555.71	0.094 68	1.4385	0.074 32	1.2×10^2	0.1018	0	57.2
0.561	1570.72	0.095 65	1.4237	0.073 35	1.9×10^6	0.1009	0	56.2
0.559	1573.75	0.095 84	1.4208	0.073 16	1.1×10^7	0.1007	0	56.0
0.555	1579.83	0.096 23	1.4150	0.072 77	3.4×10^8	0.1003	0	55.6
0.553	1582.87	0.096 42	1.4121	0.072 58	1.8×10^9	0.1001	0	55.4
0.541	1601.25	0.097 60	1.3952	0.071 40	1.4×10^{13}	0.0989	0	54.2
0.539	1604.32	0.097 79	1.3924	0.071 21	5.6×10^{13}	0.0987	0	54.0
0.537	1607.4	0.097 99	1.3896	0.071 01	2.1×10^{14}	0.0985	0	53.8
0.535 ^c	1610.47	0.098 19	1.3869	0.070 81	7.6×10^{14}	0.0983	0	53.6
0.533	1613.55	0.098 39	1.3842	0.070 61	2.7×10^{15}	0.0981	0	53.4
0.532	1615.08	0.098 49	1.3828	0.070 51	5.0×10^{15}	0.0980	0	53.3
0.531	1616.62	0.098 59	1.3815	0.070 41	9.2×10^{15}	0.0979	0	53.2
0.521	1631.97	0.099 59	1.3683	0.069 41	2.7×10^{18}	0.0969	3.0×10^{-185}	52.2
0.501	1662.37	0.101 62	1.3433	0.0673 8	3.1×10^{22}	0.0949	5.4×10^{-77}	50.2
0.481	1691.99	0.103 71	1.3203	0.065 29	4.4×10^{25}	0.0928	3.8×10^{-30}	48.2
0.451	1734.29	0.106 91	1.2897	0.062 09	1.4×10^{29}	0.0896	2.1×10^2	45.2

^a Interfacial tension between Na_2SO_4 nuclei and mixed solution. ^b Interfacial tension between NaCl and mixed solution. ^c Water activity at efflorescence point. ^d No nucleation rate because saturation is not reached yet.

TABLE 3: Comparison for ERH between Prediction and Experimental Data Obtained in This Study^a

x_β	residence time (s)	experimental ERH (%)	calculated ERH (%)	$ \Delta\text{ERH} ^b$	J_β (m ⁻³ s ⁻¹)	J_α (m ⁻³ s ⁻¹)
1.00	94	60.0 \pm 2.1	59.0	1.0	1.1×10^{19}	
0.75	89	57.9 \pm 2.2	57.2	0.7	1.0×10^{20}	
0.67	86	56.6 \pm 2.0	56.4	0.2	1.3×10^{20}	
0.50	84	54.0 \pm 2.1	53.9	0.1	1.0×10^{20}	1.7×10^{-129}
0.33	75	50.0 \pm 2.0	49.3	0.7	1.8×10^{20}	1.3×10^3
0.25	72	47.8 \pm 2.1	45.5	2.3	1.5×10^{20}	8.4×10^{18}
0.20	73	44.9 \pm 2.1	45.2	0.3	5.3×10^{12}	7.6×10^{19}
0.10	73	44.6 \pm 2.0	45.4	0.8	8.0×10^{-132}	9.6×10^{19}
0.00	78	45.1 \pm 2.2	45.7	0.6		5.5×10^{19}

^a The calculated nucleation rates of two salts at ERH are also shown. ^b The difference between experimental and calculated values.

triplicate measurements and the precision of the hygrometer, were smaller than 2.2% RH.

To examine the accuracy of the compositions of prepared solutions, we used ion chromatography (IC2690, Waters, USA) to measure the mole fraction of Na_2SO_4 and determine the standard deviation from three mixed solutions at a prescribed composition. The standard NaCl and Na_2SO_4 solutions with concentrations of 5, 25, 50, and 100 ppm were utilized to establish the calibration curves.

4. Results and Discussions

Table 3 lists the experimentally obtained ERHs of mixed NaCl– Na_2SO_4 particles (40–49 nm) at nine different Na_2SO_4 mole fractions (x_β) along with corresponding residence times determined based on the flow rates operated in this study. With the use of the listed residence times, the theoretically calculated ERHs are shown in the fourth column (Table 3) incorporating the corresponding calculated homogeneous nucleation rates for the two salts (last two columns, Table 3). As mentioned in section 2, since the residence times, instead of actual induction times, are adopted in this study, the predicted ERHs may be higher than the real values.¹ As shown in Table 3, the difference in ERH between the predicted and experimentally measured values (the fifth column) is smaller than 1% RH except for $x_\beta = 0.25$ with a discrepancy of 2.3% RH. Our theoretical prediction satisfactorily delineate experimentally observed variation in ERH as shown in Figure 2, where the experimentally

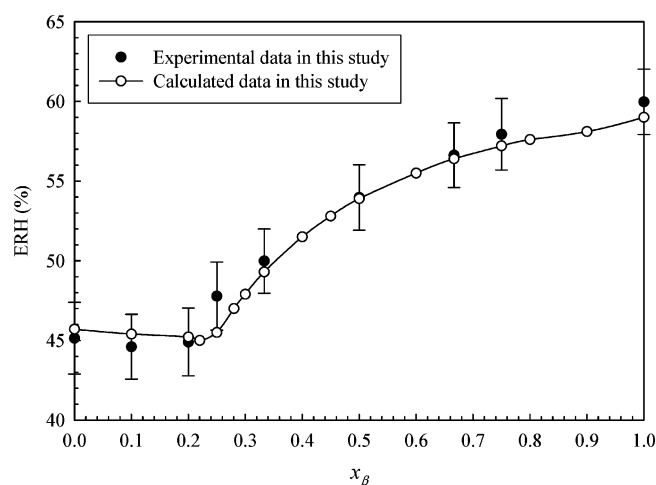


Figure 2. Variation of ERH with the mole fraction of Na_2SO_4 (x_β) for mixed NaCl– Na_2SO_4 particles with average dry-state diameter of 45 nm.

measured ERH first decreases slightly with x_β , reaches a weak minimum at $x_\beta = 0.1$, and then increases. Interestingly, $x_\beta = 0.1$ is the eutonic composition for MDRH obtained both experimentally⁶ and theoretically.⁸ It should be noted that solute nucleation is a stochastic process caused by thermal fluctuation of a supersaturated state, and therefore the induction time for a huge number of particles represents only an average value.³² At a given RH, some particles can likely effloresce in a time shorter than this mean value. In our experiments, such behavior could be reflected by a small peak indicative of a smaller size next to the major peak in the particle size distribution curve, when RH is decreased to about 1 or 2% RH higher than the ERH value for the majority of particles. The particle number ratio of the major to small peak is about 9, suggesting that a small portion of particles effloresce earlier.

To further verify our theoretical formulation, we compare theoretically calculated ERH of mixed NaCl– Na_2SO_4 particles with a dry-state diameter of 1 μm to the experimentally measured data for particles of 0.6–1.3 μm , by Lee and Chang using gas chromatography equipped with a thermal conductivity detector (GC-TCD).⁷ ERHs extracted from the results reported by Lee and Chang (Table 4) are similar to that obtained from

TABLE 4: ERH Comparison between Prediction and Experimental Data^a of Lee and Chang⁷

x_β	experimental		calculated	$ \Delta\text{ERH} ^c$	J_β ($\text{m}^{-3} \text{s}^{-1}$)	J_α ($\text{m}^{-3} \text{s}^{-1}$)
	ERH (%) ^b	ERH (%)				
1.00	58	58.1	0.1	1.2×10^{15}		
0.90	59	57.8	1.2	5.1×10^{14}		
0.75	58	56.8	1.2	7.8×10^{14}		
0.70	58	56.4	1.6	6.0×10^{14}		
0.50	53	53.6	0.6	7.6×10^{14}	0	
0.25	48	45.5	2.5	5.8×10^{14}	3.2×10^{12}	
0.10	47	45.7	1.3	1.0×10^{-269}	6.8×10^{14}	
0.00	48	46.4	1.6		4.6×10^{14}	

^a Residence time = 15 min. The calculated nucleation rates of two salts at ERH are also shown. ^b Data are extracted from the figures reported by Lee and Chang (2002).⁷ ^c Difference between experimental and calculated values.

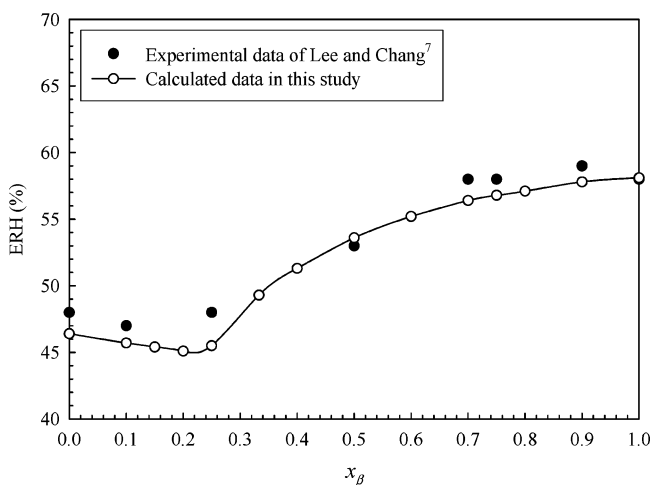


Figure 3. Variation of ERH with the mole fraction of Na_2SO_4 (x_β) for mixed NaCl – Na_2SO_4 particles with dry-state diameters of $1 \mu\text{m}$ and residence time of 15 min. The experimental data are extracted from the work of Lee and Chang.⁷

our experiments (Table 3). In addition, our theoretical prediction is in reasonable agreement with their data although the largest discrepancy (2.5% RH) between prediction and experiment measurements again occurred at $x_\beta = 0.25$ (Table 4 and Figure 3). To make further comparison, we calculated for $6 \mu\text{m}$ particles with $x_\beta = 0.5$ and obtained an ERH of 54% RH, which also concurs with the experimental value of $53 \pm 2\%$ observed by Tang.⁴

All the above comparisons indicate that the theoretical model in this study is capable of predicting the ERHs of mixed NaCl – Na_2SO_4 particles except for the composition around $x_\beta = 0.25$. To investigate possible reasons causing the deviation of predicted ERH for this composition, we examine the calculated nucleation rates J_α and J_β for the two salts (Tables 3 and 4) when the mixture particles effloresce. Except for $x_\beta = 0.25$, the nucleation rate of one salt is much higher than that of the other; the rate ratio is at least of 7 orders of magnitude. The nucleation of Na_2SO_4 greatly outpaces that of NaCl for $x_\beta > 0.25$ and vice versa for $x_\beta < 0.25$ (Tables 3 and 4). This justifies the assumption made in our formulation that each salt undergoes homogeneous nucleation separately at an early stage, and successful nucleation leading to ensuing crystal growth requires nuclei at a critical size. Since one salt nucleates and forms critical nuclei much faster, the other salt could undergo heterogeneous nucleation with the crystal of the first salt as a substrate. Therefore, the formation of critical nuclei of the first salt is the rate-controlling process for the experimentally observed efflorescence. Accordingly, the first salt shall appear

TABLE 5: Variation of Predicted ERH with Dry Diameter of Mixed NaCl and Na_2SO_4 Particles (Residence Time Is 15 Min)

x_β	ERH (%)					ΔERH^a
	particle diameter					
	$1 \mu\text{m}$	100 nm	40 nm	20 nm	10 nm	
1.00	58.1	57.8	59.2	62.0	68.7	9.5
0.90	57.8	57.6	58.8	61.7	68.3	9.5
0.75	56.8	56.6	57.9	60.7	67.2	9.3
0.50	53.6	53.5	54.6	57.2	63.2	8.6
0.10	45.7	45.3	46.0	48.0	52.6	6.6
0.00	46.4	45.7	46.5	48.1	52.3	5.8

^a Difference in ERH between 10 nm and 40 nm particles, ($\text{ERH}_{10\text{nm}} - \text{ERH}_{40\text{nm}}$).

in the core of the formed dry particle with the second salt enriched over the surface layer.¹³ For the case of $x_\beta = 0.25$, however, the ratio of nucleation rate of Na_2SO_4 to NaCl becomes smaller than 200 (Table 4) or even down to less than 20 (Table 3). Relative to the experimental data, the noticeable underestimation of the predicted ERH could be justified by two possible reasons. First, it implies that the above mentioned process may be less than applicable to predict ERH around this composition. A proposed scenario is as follows. When the homogeneous nucleation rates of two salts become sufficiently close, nuclei of one salt smaller than their critical sizes, which can form and disappear constantly, may suffice to trigger heterogeneous nucleation of the other salt, and vice versa. This is in contrast to the necessity of formation of nuclei larger than the critical size as seeds for ensuing heterogeneous nucleation, a central assumption in our formulation. Since overcoming the energy barrier estimated from the homogeneous nucleation is not required, crystallization can take place at a RH higher than predicted values obtained based on the formulation in the present study. In this case, the effloresced dry particles could consist of a homogeneous mixture. The second possible reason is the inadequacy of the empirical mixing rule of activities (eq 4) ignoring the interactions of the two solutes, which become important at high concentrations because of the nonlinear nature of sodium sulfate. The inaccuracy in the calculated water activity could be significant in particular for $x_\beta \sim 0.25$, where the ionic strengths of the two solutes are comparable.^{33,34} With the limited experimental data, we attempt to estimate the range for x_β , within which our prediction for ERH may not be as accurate. To take into account the composition precision for prepared samples, we used the IC method to test the prepared mixed solutions with x_β values of 0.2, 0.25, and 0.33 (three solutions for each of the mole fractions) and obtained the standard deviation of 0.011, 0.016, and 0.038, respectively. Hence, this range is crudely estimated to be from 0.18 to 0.37.

Because our theoretical model takes into account the Kelvin effect, the dependence of ERH on particle size is also theoretically examined. Since ERH decreases with decreasing residence time, a constant residence time of 15 min is employed, as an example, to calculate ERHs. Table 5 shows that ERH decreases when particle size decreases from $1 \mu\text{m}$ to 100 nm, while a reverse trend is seen for smaller particles ($< 100 \text{ nm}$). For all mixing ratios, the difference of ERH over particle size range 40 nm– $1 \mu\text{m}$ is no more than 1.4% RH. Such a small difference is difficult to be verified through experimental measurements, which usually have errors of at least 2% RH. Similar to the experimental observation of Biskos et al.,³⁵ the ERH increase with decreasing dry diameter starts when the particle size has been decreased to 40 nm. The increase becomes substantial in particular for particles smaller than 20 nm. We find that the

TABLE 6: Variation of Predicted ERH with Residence Time for Mixed NaCl and Na₂SO₄ Particles with a Dry Diameter of 45 nm and $x_\beta = 0.5$

t (s)	0.1	1	10	20	40	60	80	100	1200	3600
ERH (%)	52.4	53	53.5	53.6	53.7	53.9	53.9	53.9	54.4	54.6

TABLE 7: Variation of ERH with $\sigma_{\text{nuc-air}}$ for Mixed NaCl and Na₂SO₄ Particles with a Dry Diameter of 45 nm (Residence Time Is 60 s)

x_β	$\sigma_{\text{nuc-air}} (\alpha/\beta)$				
	0.183/0.155 ERH (%)	0.190/0.162 ERH (%)	0.197/0.169 ERH (%)	0.204/0.176 ERH (%)	0.211/0.183 ERH (%)
0.1	49.2	47.1	45.3	43.1	40.8
0.5	59.0	56.4	53.9	51.1	48.4

differences in ERH between 10 and 40 nm are more than 5.8% RH, and the difference increases with increasing Na₂SO₄ mole fraction as shown in the last column of Table 5. The greater increase in ERH for an increased Na₂SO₄ fraction is attributed to the higher water activity for Na₂SO₄ than for NaCl, because the exponential factor representing the Kelvin effect in eq 24 is comparable for Na₂SO₄ and NaCl at a given dry diameter from our calculation.

Finally, we address the sensitivity of predicted ERH to residence time and to surface tension between nuclei and air. In principle, the nucleation induction time could be approached experimentally by gradually reducing the residence time and monitoring the occurrence of efflorescence at a fixed RH. This can be done, for example, with a well designed exposure chamber having an adjustable length. Unfortunately, the chamber used in the present study lacks this flexibility. To examine the sensitivity of the current model to the residence time, we choose a 45 nm mixed particle with $x_\beta = 0.5$ to calculate the ERH using different values for the residence time, and the results are shown in Table 6. It is found that the current model for mixed Na₂SO₄–NaCl particles is not so sensitive to the residence time ranging widely from 0.1 to 3600 s. The sensitivity of predicted ERH to the surface tension between nuclei and air ($\sigma_{\text{nuc-air}}$) is analyzed by making the surface tension deviate slightly away from the inferred $\sigma_{\text{nuc-air}}$ (0.197 and 0.169 N/m for NaCl and Na₂SO₄). The results in Table 7 indicate that our prediction is strongly sensitive to $\sigma_{\text{nuc-air}}$. Since $\sigma_{\text{nuc-air}}$ is used to calculate $\sigma_{\text{nuc-drop}}$, a change in $\sigma_{\text{nuc-air}}$ can considerably alter the Gibbs energy (eq 2) and then the ERH. Therefore, an accurate experimental measurement for $\sigma_{\text{nuc-air}}$ is critical for validation of the present formulation.

5. Conclusion

Our theoretical model is built to predict the ERHs of particles containing mixed NaCl and Na₂SO₄ at various molar ratios and shows satisfactory agreement with experimental values, except for the cases with a Na₂SO₄ mole fraction of around 0.25. The general agreement supports our hypothesis that for mixed salt particles, efflorescence is controlled by the homogeneous nucleation of one salt, whose nucleation rate is far much higher than that of the other. However, at mixing ratios where the individual nucleation rates of two salts are close enough to each other, our theoretical formulation underestimates ERH as compared to the experimental data. For this unique case, the attribution is twofold: (1) the hypothesized mechanism, homogeneous nucleation of one salt followed by heterogeneous nucleation, cannot well describe the efflorescence process and requires further investigation; (2) the mixing rule of activities used is inadequate for accurate prediction. Relative to particles larger than 40 nm, the Kelvin effect plays an important role in

the ERHs of mixed NaCl–Na₂SO₄ particles smaller than 40 nm and becomes substantial for sizes below 20 nm. In addition, the higher the Na₂SO₄ mole fraction, the larger the increase in ERH.

Acknowledgment. The authors are grateful to the financial support from National University of Singapore through Grants R-279-000-203-112 and R-288-000-026-133.

Appendix: Empirical Equations for Molality and Density of Pure Salt Solutions

For pure salt solutions, the salt molalities are given by

$$m_\alpha = 2476.8287a_w^6 - 9150.69602a_w^5 + 13570.04362a_w^4 - 10377.69477a_w^3 + 4378.89202a_w^2 - 1022.46916a_w + 125.23519 \quad (\text{A1})$$

$$m_\beta = 985.27913a_w^4 - 3450.21842a_w^3 + 4474.50201a_w^2 - 2569.42664a_w + 559.83158 \quad (\text{A2})$$

The densities are estimated by

$$\rho_\alpha = (0.99845 + 6.9599 \times 10^{-3}wf_\alpha + 2.58586 \times 10^{-5}wf_\alpha^2) \times 1000 \quad (\text{A3})$$

$$\rho_\beta = (0.9971 + 8.871 \times 10^{-3}wf_\beta + 3.195 \times 10^{-5}wf_\beta^2 + 2.28 \times 10^{-7}wf_\beta^3) \times 1000 \quad (\text{A4})$$

where

$$wf_i = 100 \frac{M_{\text{salt},i}m_i}{1000 + M_{\text{salt},i}m_i}$$

Equations A2 and A4 are used by Tang,⁴ eq A3 is from Hämeri et al.,³⁶ and eq A1 is a polynomial obtained by combining the work of Ally et al.³⁷ and Tang et al.,³⁸ which have all been detailed in our earlier work.³⁹

References and Notes

- (1) Gao, Y.; Chen, S. B.; Yu, L. E. *J. Phys. Chem. A* **2006**, *110*, 7602–7608.
- (2) Heintzenberg, J. Fine particles in the global troposphere, A review. *Tellus* **1989**, *41B*, 149–160.
- (3) Seinfeld, J. H.; Pandis, S. N. *Atmospheric Chemistry and Physics: From Air Pollution to Climate Change*; John Wiley: New York, 1998.
- (4) Tang, I. N. *J. Geophys. Res.* **1997**, *102*, 1883–1893.
- (5) Ha, Z.; Choy, L.; Chan, C. K. *J. Geophys. Res.* **2000**, *105*, 11699–11709.
- (6) Chang, S. Y.; Lee, C. T. *Atmos. Environ.* **2002**, *36*, 1521–1530.
- (7) Lee, C. T.; Chang, S. Y. *Atmos. Environ.* **2002**, *36*, 1883–1894.
- (8) Potukuchi, S.; Wexler, A. S. *Atmos. Environ.* **1995**, *29*, 1663–1676.
- (9) Nenes, A.; Pandis, S. N.; Pilinis, C. *Aquat. Geochem.* **1998**, *4*, 123–152.
- (10) Topping, D. O.; McFiggans, G. B.; Coe, H. *Atmos. Chem. Phys.* **2005**, *5*, 1205–1222.
- (11) Amundson, N. R.; Caboussat, A.; He, J. W.; Martynenko, A. V.; Savarin, V. B.; Seinfeld, J. H.; Yoo, K. Y. *Atmos. Chem. Phys.* **2006**, *6*, 975–992.
- (12) Schlenker, J. C.; Malinowski, A.; Martin, S. T.; Hung, H.; Rudich, Y. *J. Phys. Chem.* **2004**, *108*, 9375–9383.
- (13) Ge, Z.; Wexler, A. S.; Johnston, M. V. *J. Colloid Interface Sci.* **1996**, *183*, 68–77.
- (14) Braban, C. F.; Abbatt, J. P. D. *Atmos. Chem. Phys.* **2004**, *4*, 1451–1459.
- (15) Han, J. H.; Hung, H. M.; Martin, S. T. *J. Geophys. Res.* **2002**, *107*, 4086.
- (16) Richardson, C. B.; Snyder, T. D. *Langmuir* **1994**, *10*, 2462–2465.

- (17) Onasch, T. B.; McGraw, R.; Imre, D. *J. Phys. Chem. A* **2000**, *104*, 10797–10806.
- (18) Söhnle, O.; Garside, J. *Precipitation: Basic Principles and Industrial Applications*; Butterworth-Heinemann: Oxford, England, 1992.
- (19) Tang, I. N.; Munkelwitz, H. R. *J. Geophys. Res.* **1994**, *99*, 18801–18808.
- (20) Chan, M. N.; Lee, A. K. Y.; Chan, C. K. *Environ. Sci. Technol.* **2006**, *40*, 6983–6989.
- (21) Lide, D. R., Ed. *CRC Handbook of Chemistry and Physics*; Taylor and Francis: Boca Raton, FL, 2006; Internet version, <http://www.hbcpnet-base.com>.
- (22) Robinson, R. A.; Stokes, R. H. *Electrolyte Solutions, the Measurement and Interpretation of Conductance, Chemical Potential, and Diffusion in Solutions of Simple Electrolytes*, 2nd ed.; Butterworths: London, U.K., 1965.
- (23) Chan, C. K.; Ha, Z. *J. Geophys. Res.* **1999**, *104*, 30193–30200.
- (24) Cohen, M. D.; Flagan, R. C.; Seinfeld, J. H. *J. Phys. Chem.* **1987**, *91*, 4563–4574.
- (25) Bromley, L. A. *AIChE J.* **1973**, *19*, 313–320.
- (26) Kusk, C. L.; Meissner, H. P. *AIChE Symp. Ser.* **1978**, *173*, 14–20.
- (27) Kim, Y. P.; Seinfeld, J. H.; Saxena, P. *Aerosol Sci. Technol.* **1993**, *19*, 157–181.
- (28) Yu, Y. X.; Gao, G. H.; Daridon, J. L.; Lagourette, B. *Fluid Phase Equilib.* **2003**, *206*, 205–214.
- (29) Hu, Y. F.; Lee, H. *J. Colloid Interface Sci.* **2004**, *269*, 442–448.
- (30) Pruppacher, H. R.; Klett, J. D. *Microphysics of Clouds and Precipitation*; D. Reidel: Dordrecht, Holland, The Netherlands, 1978.
- (31) Li, Z. B.; Li, Y. G.; Lu, J. F. *Ind. Eng. Chem. Res.* **1999**, *38*, 1133–1139.
- (32) Olsen, A. P.; Flagan, R. C.; Kornfield, J. A. *Rev. Sci. Instrum.* **2006**, *77*, 073901.
- (33) Chan, C. K.; Liang, Z.; Zheng, J.; Clegg, S. L.; Brimblecombe, P. *Aerosol Sci. Technol.* **1997**, *27*, 324–344.
- (34) Clegg, S. L.; Brimblecombe, P.; Liang, Z.; Chan, C. K. *Aerosol Sci. Technol.* **1997**, *27*, 345–366.
- (35) Biskos, G.; Malinowski, A.; Russell, L. M.; Buseck, P. R.; Martin, S. T. *Aerosol Sci. Technol.* **2006**, *40*, 97–106.
- (36) Hämeri, K.; Laaksonen, A.; Väkevä, M.; Suni, T. *J. Geophys. Res.* **2001**, *106*, 20749–20757.
- (37) Alty, M. R.; Clegg, S. L.; Braunstein, J.; Simonson, J. M. *J. Chem. Thermodyn.* **2001**, *33*, 905–915.
- (38) Tang, I. N.; Munkelwitz, H. R.; Wang, N. *J. Colloid Interface Sci.* **1986**, *114*, 409–415.
- (39) Gao, Y.; Chen, S. B.; Yu, L. E. *Atmos. Environ.* **2007**, *41*, 2019–2023.